



Optimum Design of Liquefied Natural Gas Bi-lobe Tanks using Finite Element, Genetic Algorithm and Neural Network

Mohammadreza Salarkia¹, Sa'id Golabi², Behzad Amirsalari³

¹ Department of Mechanical Engineering, The University of Kashan, Kashan, 8731753153, Iran, Email: mssalarkia@gmail.com

² Department of Mechanical Engineering, The University of Kashan, Kashan, 8731753153, Iran, Email: golabi-s@kashanu.ac.ir

³ Department of Mechanical Engineering, The University of Kashan, Kashan, 8731753153, Iran, Email: amirsalari.behzad@gmail.com

Received August 11 2019; Revised October 07 2019; Accepted for publication October 07 2019.

Corresponding author: Sa'id Golabi (golabi-s@kashanu.ac.ir)

© 2020 Published by Shahid Chamran University of Ahvaz

& International Research Center for Mathematics & Mechanics of Complex Systems (M&MoCS)

Abstract. A comprehensive set of ten artificial neural networks is developed to suggest optimal dimensions of type 'C' Bi-lobe tanks used in the shipping of liquefied natural gas. Multi-objective optimization technique considering the maximum capacity and minimum cost of vessels are implemented for determining optimum vessel dimensions. Generated populations from a genetic algorithm are used by Finite Element Analysis to develop new models and find primary membrane and local stresses to be compared with their permissible ranges using PYTHON coding. The optimum design space is mathematically modeled by training ten artificial neural networks with design variables generated by the Taguchi method. The predicted results are compared with actual design data and the 93% achieved accuracy shows the precision of the developed design system.

Keywords: Liquefied Natural Gas, Bi-lobe tank, Finite Element Method, Genetic algorithm, Artificial Neural Network, Taguchi method.

1. Introduction

Without any doubt and by increasing energy demand, Natural gas (NG) is pronounced a perfect option for bridging the gap between the current energy market with pollutant fuels and the next decade's new energies [1]. Natural gas is also recognized as an environmentally friendly [2, 3], economical [4, 5], safe [6, 7] and clean [8, 9] fuel with lower emissions (NOX, SOX, ...) in comparison with heavy fuel oil (HFO) and other relevant fuels. The remarkable issue about NG is the increasing demand for Liquefied Natural Gas (LNG) in the global market, which makes it one of the fastest-growing and issues in the energy industry [1]. Recently, due to many superiorities from environmental and economic aspects, LNG and its related issues has attracted the attention of many scientists regarding LNG market and trading [10, 11]; transport section including railroad [12, 13], road [14, 15] and heavy-duty vehicle [16]; marine transportation [17, 18], infrastructure and its impact [19-21]; gas station [22]; LNG Tankers [23-25] and cargo containment system [26-28]; and LNG tank design [29, 30]. Because of significant reduction of volume, transportation of NG in liquefied states, i.e., Liquefied Natural Gas (LNG) and Liquefied Petroleum Gas (LPG) [31] by specific ships (Liquefied Gas Tankers or Gas Carriers) increases the economic advantages of using these fuels [32]. Thus, from the transportation point of view and due to the special properties of LNG, the affordable and economical way to transport LNG is using cargo ships. Meanwhile, regarding the widespread consumption of LNG as an appropriate alternative fuel [33] and dramatic increase of energy demand in one hand, and its sufficient accessible resources considering current production rate, on the other hand, gas fuel will last over 50 years more than oil (52.5 years). Hence, considering the impressive changes made in LNG equipment and construction technologies and based on the International Energy Agency estimation, there is sufficient supply for 250 years of consumption [33-35], and by considering the impressive changes made in LNG equipment and construction technologies, the necessity for

scrutinizing LNG fuel tanks and carriers looks more and more inevitable [18-21]. Generally, various types of tanks with different capacities are used for transporting LNG including prismatic, spherical, membrane, semi-membrane and independent tanks [36]. On the other hand, there are 3 independent types of tanks including Type 'A, B, and C'; while type 'C' also is divided into 3 subtypes: Cylindrical, Bi-lobe and Tri-lobe. According to IMO¹, type 'C' tanks are more safe and reliable, with easier fabrication and installation process [37, 38]. Independent type 'C' tanks are flexible and competitive, and the demand for small and medium LNG carriers have been increased for coastal operation, nowadays [30]. The flexibility of this type of vessel during Boiling of Gas (BOG) and its pressure management zone accompanied by the fact that no secondary barrier is required for them, increase the interest of industrial authorities for utilizing them. Hence, Wang et al. [39] studied the strength evaluation of independent Type 'C' LNG carriers using finite element method (FEM). They analyzed bi-lobe tanks and their major components including tank shell, longitudinal central bulkhead, stiffener rings, and saddle supports, considering ASME² Boiler and Pressure Vessel (BPV) [40] requirements and IGC³ codes [41]. Buckling of bi-lobe tanks under external pressure was studied and a complete procedure for evaluating the structural strength of a tank and its other accessories was derived. The analysis of spherical type LNG tanks under diverse static loads was also addressed by Shin and Ko [23]. Stress analysis of saddle support for horizontal pressure vessels was addressed by Kumar et al. [42] using ANSYS software and applying the mathematical method based on ASME BPV codes [40]. Yao et al. [43] determined the thickness of various parts of type 'C' LNG tank by implementing ANSYS FEM software under various loads. Shin et al. [44] used ASME Sec VIII Div. 2, IMO and IGC codes [41] to design a type 'C' LNG fuel storage tank with capacity of 500 m³. Senjanović et al. [45] requested for a remedy for misalignment of bi-lobe tank heads in LPG carriers. The results of their research indicated that the reason for this unwanted phenomenon is the high-stress concentration that occurs in Y-joint.

Bi-lobe tanks have also two great privileges compared with cylindrical tanks including; lower construction cost than that of 2 individual cylindrical tanks with the same volume, and lower occupied space than 2 individual vessels, considering the need for respecting minimum standard space between two cylinders. Hence, because of increasing interest in the application of bi-lobe tanks, this paper scrutinized the optimum design of type 'C' LNG Bi-lobe tanks, used for carrying and transporting LNG by ships and marine transport sector. Accordingly, no comprehensive study has been found in the literature that addresses the optimum design of LNG Bi-lobe tank design. Considering an available space for installing an LNG tank, there is no code or approved procedure for designing optimum vessel dimensions. Here, a comprehensive design methodology was presented for determining the optimum dimension of bi-lobe tanks for various available spaces. In other words, considering width, length, and height of available space in a ship, determining optimum dimensions of a bi-lobe with maximum capacity and minimum cost has not been addressed before. Hence, by considering codes and standards, design conditions, construction method and determining other technical parameters such as mechanical properties of proposed material (AISI 304L) at the specific working temperature; optimal design of Bi-lobe tanks has been studied by simultaneous employing FEM and Genetic Algorithm (GA) optimization method. The aim of this multi-objective optimization problem was to concurrently increase tank capacity and reduce its construction cost. Subsequently, it was shown that how the results of 144 designed cases were used to train a set of accurate Artificial Neural Networks (ANN) and develop an applicable tool for designing an optimum bi-lobe for any specific space.

2. Methodology

A type 'C' Bi-lobe tank can be imagined as two horizontal cylindrical tanks joined together as shown in Fig. 1). This vessel can be defined by its major dimensions: shell length (l'), body radius (r), and deviation of each tank from the symmetry plane (a). Therefore, the total length (l) and width (w) of the vessel can be calculated as follows:

$$l = l' + 2r \quad (1)$$

$$w = 2(r + a)$$

Initially, the dimensional constraints of Bi-lobe tanks were selected as variables based on desired tank volume and their dimensional ratios. To meet relevant tank installation location and ship dimensions mandatory IGF⁴ codes [46], and to guaranty independency of tank design from rules, regulations and restrictions; these constraints, as ships' installation space, were presumed as hypothetical rectangular cubes (HRC) whose sides (L , H , and W) act as upper limits for designed tanks outer dimensions (l , h , and w). In other words, it is required to determine optimum dimensions of a Bi-lobe, i.e. l , h , and w , that can be inscribed in a rectangular cube with length L , height H and width W (Fig. 1).

After determining the levels of an experiment for volume and dimensional ratios of HRC and saddle angles, 72 cases for constraints were created by the factorial method. Afterward, the multi-objective optimization function was proposed to maximize tank capacity and minimize construction cost, simultaneously. Hence, considering 2 different states of cost-to-volume importance factors (IF), 144 cases were analyzed and optimized by integration of FEM and GE. Eventually, the optimum outputs, including best dimensions and objective functions, were separately used for training 10 ANNs, whose

¹ International Maritime Organization (IMO)

² the American Society of Mechanical Engineers (ASME)

³ International Gas Carrier (IGC)

⁴ International Code for Ships Fuelled by Gases or Other Low-Flashpoint Fuels (IGF)



best architectural structure was selected by Taguchi Design of Experiments (DOE) algorithm, to comprehensively forecast the feasible region of optimal design. The schematics of this trend is illustrated in Fig. 2.

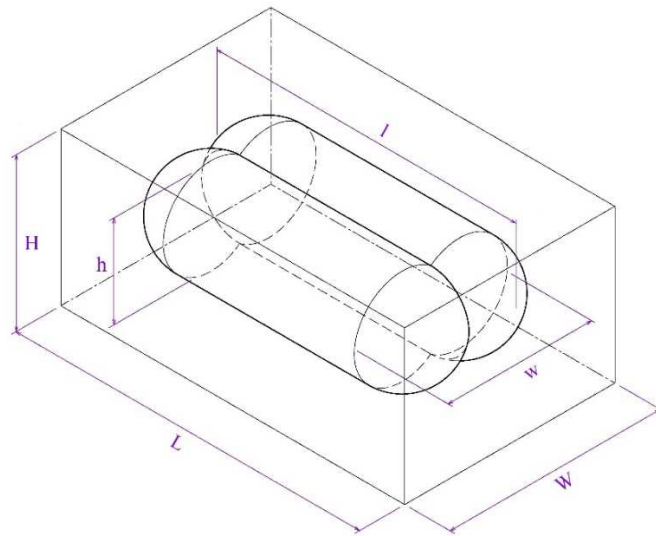


Fig. 1. Schematics of a Bi-lobe tank inscribed in HRC

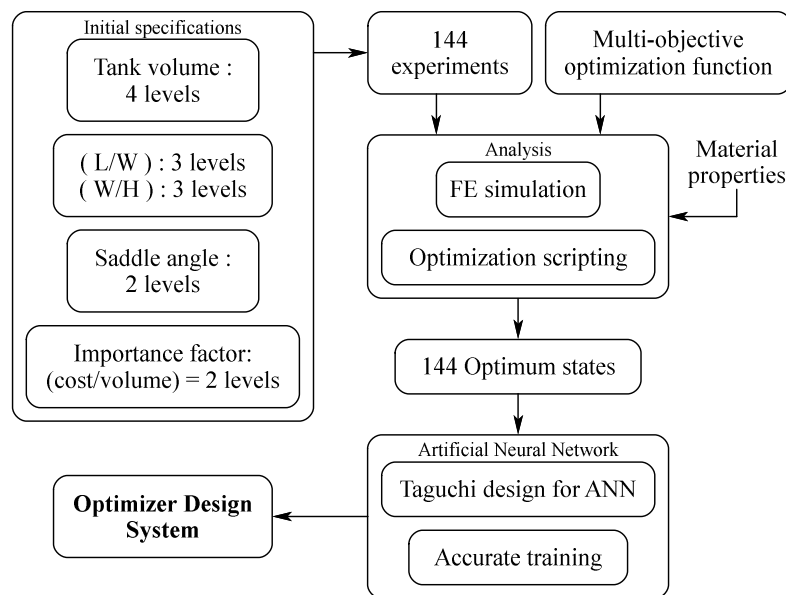


Fig. 2. Methodology schematics

Before any attempt for generating a method for determining bi-lobe tanks optimum design and parameters, design parameters, constraints, and objectives are needed to be specified.

At the design temperature of -163°C , the design vapor pressure of type ‘A’ tanks -considered as atmospheric tanks- is less than 0.7bar, while it is about 4.5 bar for independent type ‘C’ Bi-lobe tanks. At this temperature, the total carrying capacity for ships with 3 and 4 Bi-lobe tanks is about 25000m³ and 35000m³ respectively [47]. Thus, to cover all considerable volumes and acceptable dimensions, the desired volume range of HRC, in which tanks are inscribed, is considered between 500 to 9000m³. This continuous range of volume should be covered appropriately in this study. Therefore, to reach a finite number of problems, 4 amounts out of this range were considered in this research. Besides, to cover various dimension ratios, every volume was considered for 9 different dimensional ratios (Table 1). These ratios were selected deliberately to omit large and small ratios of L/W and W/H that lead to thin shells with low volume or thick shells with high cost.

Table 1. Levels of change for dimensional constraints

Variable	Levels of change
Volume (m ³)	500, 3000, 6000, 9000
L/W	2, 3, 4
W/H	1, 1.5, 2

Hence, 36 various sets of dimensions were specified (Table 2) and each was utilized in 4 different optimization problems considering 2 different saddle angles based on relevant codes [48], i.e. 120° or 150° [48] and 2 diverse cost-to-volume IF ratios, i.e. $\alpha/\beta = 0/1$ and 0.2/0.8. Obviously, when using 0 for cost the main objective was to just consider maximum volume during optimization. On the other hand, during considering 0.2 for cost and consequently 0.8 for volume, the effect of the cost was a little increased during optimization. The reason for delimiting IF between these two amounts is that; further increasing cost IF did not lead to any better design parameters since the effect of maximum volume during optimization was more important than the effect of cost for a ship. On the other hand, values of volume IF out of this specified range led to a point where tank's volume was very small and unreasonable. Consequently, the optimization problem were solved for 144 cases via a super-computer by implementing GA optimization in the ABAQUS environment using PYTHON scripting. In this study, whole calculations were thoroughly based on three-dimensional FEM analysis performed according to standard design specifications of LG¹ carrier ships and IGC code [41] requirements.

Table 2. Factorial design of geometrical constraints

No.	V (m ³)	W (m)	H (m)	L (m)	No.	V (m ³)	W (m)	H (m)	L (m)
1	500	6.3	6.3	12.6	19	6000	14.4	9.6	43.3
2	3000	11.4	11.4	22.9	20	9000	16.5	11.0	49.5
3	6000	14.4	14.4	28.8	21	500	5.7	3.8	22.9
4	9000	16.5	16.5	33.0	22	3000	10.4	6.9	41.6
5	500	5.5	5.5	16.5	23	6000	13.1	8.7	52.4
6	3000	10.0	10.0	30.0	24	9000	15.0	10.0	60.0
7	6000	12.6	12.6	37.8	25	500	7.9	4.0	15.9
8	9000	14.4	14.4	43.3	26	3000	14.4	7.2	28.8
9	500	5.0	5.0	20.0	27	6000	18.2	9.1	36.3
10	3000	9.1	9.1	36.3	28	9000	20.8	10.4	41.6
11	6000	11.4	11.4	45.8	29	500	6.9	3.5	20.8
12	9000	13.1	13.1	52.4	30	3000	12.6	6.3	37.8
13	500	7.2	4.8	14.4	31	6000	15.9	7.9	47.6
14	3000	13.1	8.7	26.2	32	9000	18.2	9.1	54.5
15	6000	16.5	11.0	33.0	33	500	6.3	3.1	25.2
16	9000	18.9	12.6	37.8	34	3000	11.4	5.7	45.8
17	500	6.3	4.2	18.9	35	6000	14.4	7.2	57.7
18	3000	11.4	7.6	34.3	36	9000	16.5	8.3	66.0

The Type of material has a great role in the design of LNG Bi-lobe tanks. 36% Ni-Fe steel, 9% Ni steel, stainless steel type AISI 304L, and Aluminum alloy type 5083 are generally used for fabricating LNG tanks at cryogenic temperature of -163°C [49]. Since austenitic stainless steel sheets SA240 -Tp 304L is the most common material used for Bi-lobe tanks, it was selected as design material in this research. The chemical and mechanical properties of 304L are presented in Table 3 and Table 4, respectively:

Table 3. Typical chemical compositions of 304L used in LNG tanks [49]

Alloy	Element (Maximum Weight %)								
	UNS	C	Si	Mn	S	P	Ni	Cr	Fe
304L	S30403	0.03	1.00	2.00	0.030	0.040	8.0-12.0	18.0-20.0	Bal

Table 4. Physical and mechanical properties of SS304L [49, 50]

Property	T °C	Value
Density (Kg/m ³)	-	7900
Elastic Modulus E (GPa)	+20	193
	-196	205
Thermal Conductivity, (w/m°C)	+20	13.4-15.1
	-196	9
Yield stress, (MPa)	0	250
	-196	400
Ultimate tensile stress, (MPa)	0	590
	-196	1525
Elongation to break, (%)	0	60
	-196	40

¹ Liquefied Gases (LG)



3. Finite Element Simulation

The main objective of using finite element technique in this research was to find the stresses at critical points during pressure loads and compare them with their permissible amounts. Accordingly, there are three important issues that must be considered in this step:

- 1- Specify the design points of Bi-lobe tanks and find the stresses in various design points.
- 2- Determine the category of stresses in design points.
- 3- Specify the permissible values for each stress categories and compare them with the stresses in design points.

Accordingly, tanks with various dimensions were needed to be simulated using FE software. These simulations were then used during optimization for determining optimum Bi-lobe parameters. Hence, a Bi-lobe tank with spherical heads, a longitudinal bulkhead, and shell reinforcing internal rings, was modeled and meshed in ABAQUS software. The element used here was S4R, i.e. a quadrilateral, stress/displacement shell element with reduced integration, whose converged size was determined during analysis. However, since optimization step was performed for various vessel sizes and it seems that for each stage of optimization convergence test should be step, mesh size was converged by considering mesh-to-tank radius ratio, instead of its size. After trying various ratios of element size to tank radius, and considering the resulted von Mises stress, this ratio was finally chosen to be 1:25. During FE analysis, tanks deadweight, weight of carrying liquid and internal pressure generated from vapor pressure and specified by USCG1 [51] and IMO [45], were the loads considered during analysis. Saddles apply reaction forces to the tank, and they have freedom of slight movement along tank axis to diminish the effect of any longitudinal thermal expansion. Thus, to simulate the effect of saddles, mechanical boundary conditions were considered to limit movements of saddle-shell contact area along transverse and vertical directions, i.e., Y and X axes respectively.

As explained in the above list, the design points, stress in design points and their categories must be calculated and specified. The design points are shown in Fig. 3. These points consist of:

a) Junctions of two surfaces where the stresses are primary local, i.e., head to head (D), shell to head (E), shell to reinforcement ring (F), and shell to shell (G).

b) Points far from junctions on the head (A), shell (B), or bulkhead (C), where the stresses are primary membrane.

The maximum amount of primary membrane stresses must not exceed permissible strength of the shell and head material at design temperature and the maximum amount of primary local stresses must be less 1.5 times permissible strength of shell material [48].

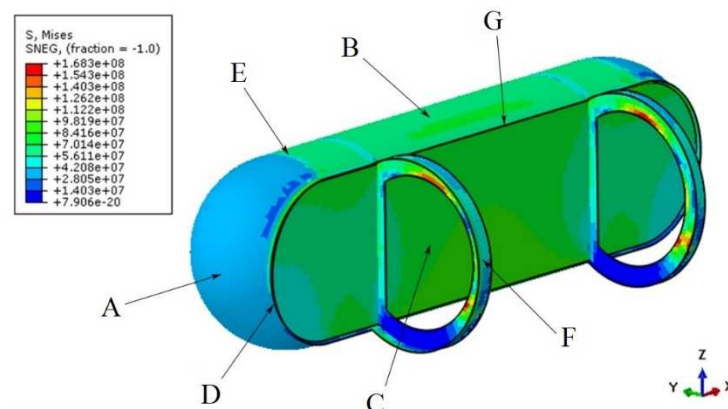


Fig. 3. Spots for reading stress on the vessel

4. Optimization

The next step for optimum design generation was a combination of GA and FEM to optimize the cases defined within the defined dimensional constraints, using Python coding. The optimization code was included in a PDE file, generated during modeling Bi-lobe tanks, for determining optimum tank dimensions shown in Fig. 4. This trend, depicted in Fig. 5., was repeated for each generated set of constraints in the previous step. The design parameters should clearly show Bi-lobe design dimensions, hence, tank radius (r), deviation from the symmetry plane (a), shell length (l), saddle angle (γ), head thicknesses (t_1), shell thickness (t_2), stiffener rings thickness (t_3), and longitudinal bulkhead thickness (t_4) are the required design parameters; while, total width (w), length (l), and height of the tank (h), are considered to be 3 of 4 inputs to the problem. To have a good image from the proposed Bi-lobe type 'C' tank, a vessel with its dimensional parameters is shown in Fig. 4.

Thereafter, the multi-objective function should be defined considering minimum construction cost and maximum capacity (volume). After a primary investigation from market and pressure vessel manufacturers, two parameters were found to be more effective on the cost of the vessel, i.e. weight and manufacturing cost. Though the price of various metals does not remain constant and many political, economic, etc. issues affect their prices, in this research the cost of SS304L at the time

of this study was considered to be 2.9 \$/Kg. Considering about 30% extra cost for manufacturing per weight of the vessel, the cost function is 1.3 times vessel weight multiplied by 2.9 \$/Kg. The cost function must be minimized while the tank volume must be maximized and these two objective functions must be considered simultaneously. On the other hand, these two functions do not have the same order and their effect on the combined objective function needed to be balanced. After getting the price of various Bi-lobe tanks from the manufacturers, it was found that 280 \$/m³ could be a suitable factor for volume function in this research. Obviously, this factor depends on material price, manufacturing costs, etc. and varies from time to time. Hence, the final objective function is defined as follows:

$$\begin{aligned} \text{Objective function } (f) &= -\alpha C + \beta V \\ &= -\alpha(\text{vessel weight} * \text{construction coefficient} * 2.9) + \beta(\text{tank volume} * 280) \end{aligned} \tag{2}$$

C and V stand for cost and volume of a tank respectively, and (α, β) are the weights or Importance Factors (IF) of cost and volume respectively, which were the 4th input to this optimization problem. These factors were considered to be (0,1) or (0.2,0.8) in this research. By using (0, 1) factors, only volume was intended to be maximized. However, considering maximum volume without including the cost of fabricating a vessel during optimization is nonsense and only maximum volume regardless of its price are investigated. On the other hand, increasing the weight of cost would lead to a tank with less volume while volume is more important than the cost and the payback time of CNG tanks is not much. Therefore, it was found that the maximum IF of 0.2 for Cost and 0.8 for volume fulfills this research’s requirements.

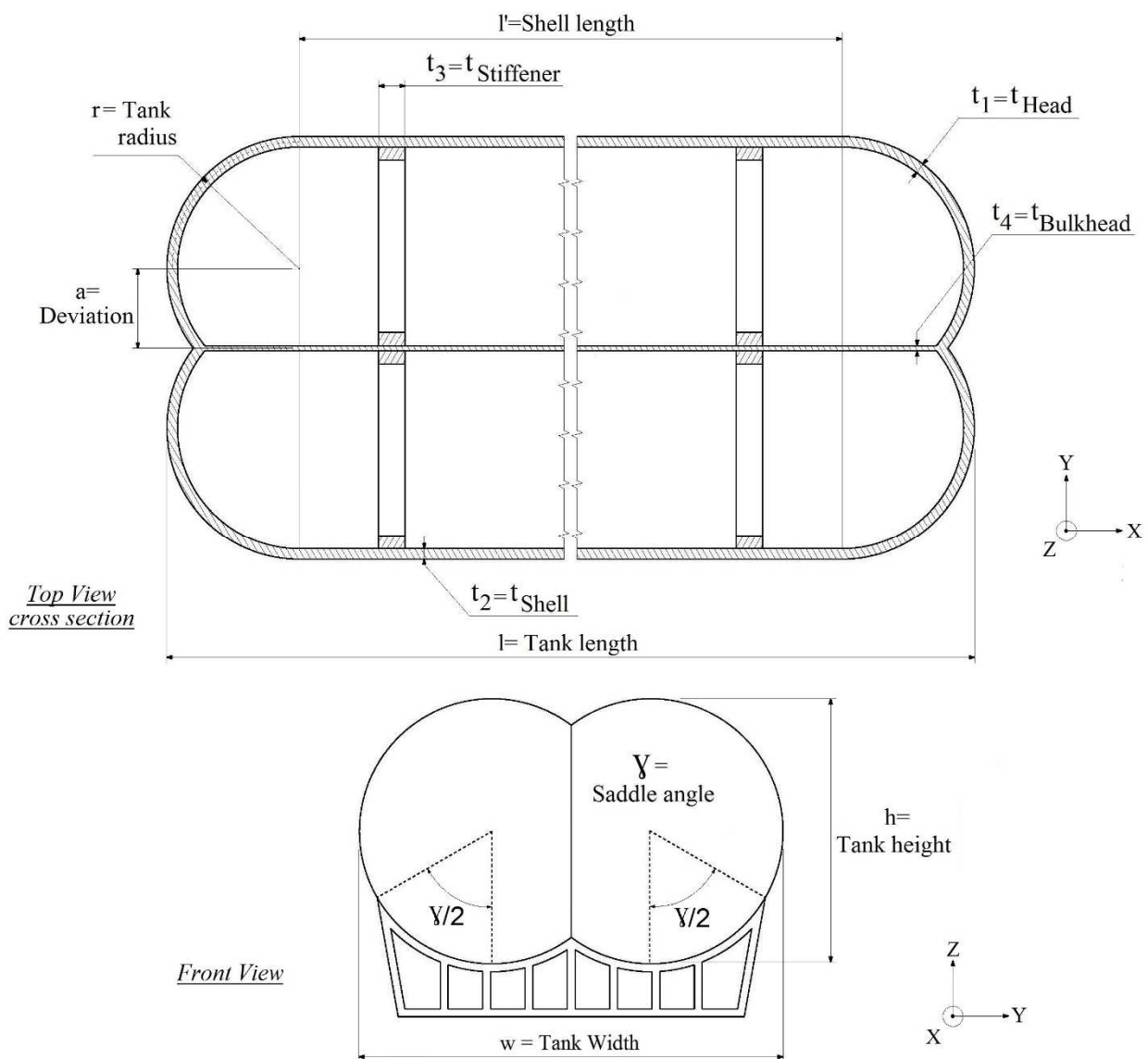


Fig. 4. Bi-lobe tank dimensional parameters

To guarantee the creation of Bi-lobe tanks with proper geometry and enough strength under loading, two sets of constraints should be satisfied during various stages of the analysis. To avoid unnecessary analyses of tanks with improper Bi-lobes dimensions, the constraints shown by Eq. (3-a). were checked immediately after the creation of a new population (Bi-lobe tank dimensions) by GA. Besides, the maximum stress in different locations of Bi-lobes was checked as specified

by constraints in Eq. (3-b). during FE analysis. The maximum limits for stress constraints were designed according to ASME Sec II, part D subpart 1 [40] at specific design temperature for two local and primary stress categories. In this research, the minimum acceptable amount of maximum stress was also considered during optimization to avoid unreasonable thicknesses especially when 0 was taken as the weight for cost in the objective function. In other words, when there is no lower limit for maximum stress, all thick dimensions for thicknesses satisfy the upper constraints which consequently increase the weight and cost of fabricating a tank. Therefore, when a lower limit is considered for maximum stresses during optimization, thick shells were rejected during analysis.

Since both primary local stresses at the two cylindrical shells or head-shell junctures, and primary membrane stresses were generated on shells or heads far from the junctures or any discontinuity (Fig. 3), it was necessary to consider the permissible strength for each separately. As explained before, this important strength limit was considered in the constraints specified in Eq. (3-b).

$$1 < w/h < 2$$

$$1 < l'/w < 3 \tag{3a}$$

$$S_{critical} (S_C) = \text{Min} \left(\frac{2}{3} S_y, \frac{S_{ut}}{3.5} \right)$$

$$0.8 S_C < S_{Primary\ membrane} < S_C$$

$$1.2 S_C < S_{Primary\ Local} < 1.5 S_C \tag{3b}$$

In the next step of analysis, a parametrically modeled Bi-lobe tank in ABAQUS finite element software was recalled and during each optimization step, the generated parameters (population) by GA were used as new parameters for the model. It should also be noted that some other necessary design constraints were considered in PYTHON coding. For example, it was considered that head thickness (t_1) cannot be lower than shell thickness (t_2), thus, t_1 is greater or equal to t_2 .

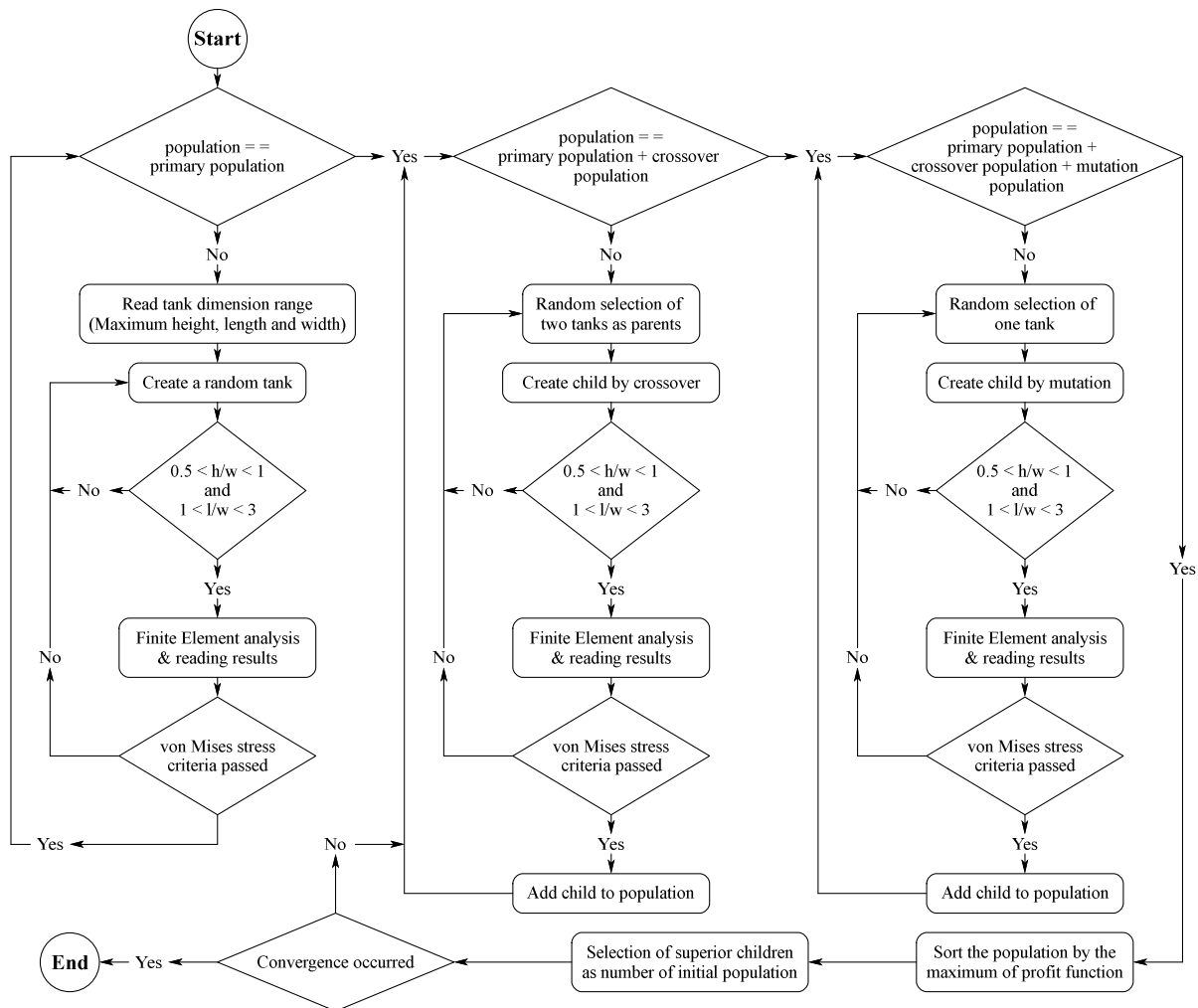


Fig. 5. Simulation and optimization trend

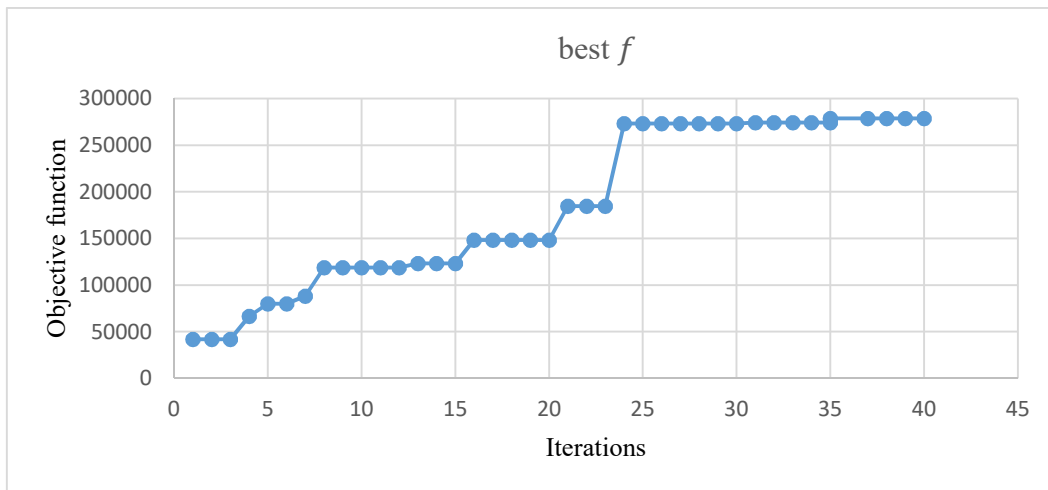


Fig. 6. Convergence diagram (optimization function)

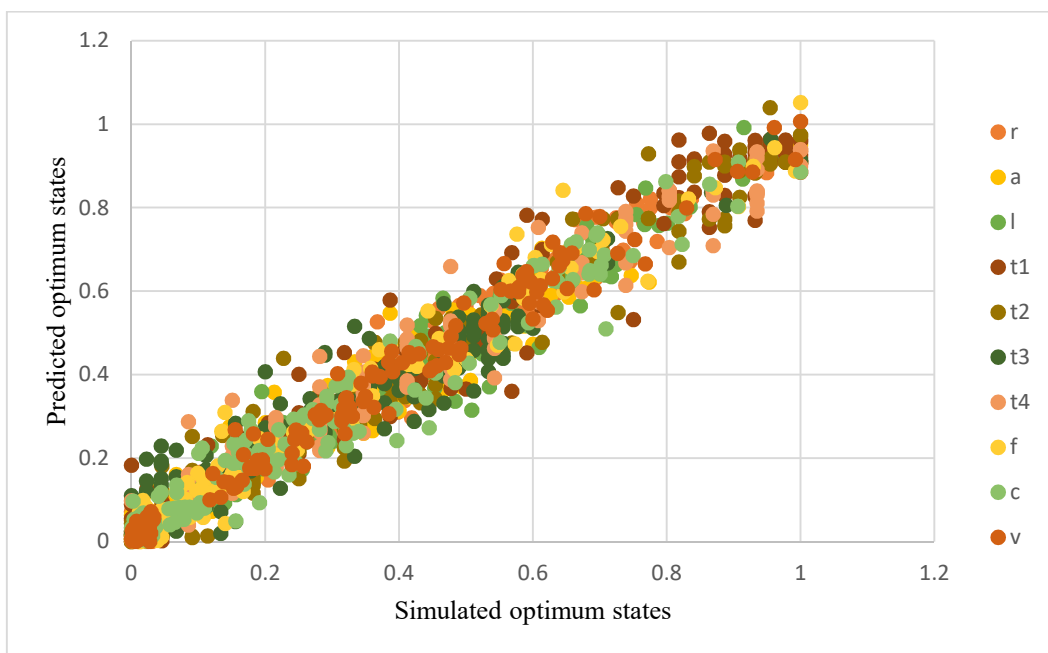


Fig. 7. Predicted vs simulated optimum outputs (normal values)

Hence, considering the depicted approach in Fig. 5, the optimization process was performed for each output individually, and the convergence trend for optimization of the objective function (f) is shown as an example in Fig. 6. Finally, during optimization, the most suitable vessel dimensions were determined for each of 144 designed experiments, and the results were shown in Table A.1 (see the Appendix A).

5. Developing Artificial Neural Networks

Since, the optimization process just presents a set of discrete optimum points, which are not capable to cover all feasible region, the ANNs were implemented to predict the whole continues region of Bi-lobe tanks design parameters. The ultimate step for developing an optimum Bi-lobe tanks design system was to train and develop ANNs for predicting design parameters for any unexperienced problem. Hence, feedforward backpropagation ANNs were used to predict unexperienced optimal states by training them with optimal modes obtained from the previous steps. The developed ANNs were used to forecast all points in the optimal feasible region, whose meticulous performance was ensured by allocating one separate network with best architectural structure to each output (design parameter). In order to attain the best possible structure for neural networks, Taguchi Design of Experiments (DoE) algorithm was used and 18 sets of ANN features for proper coverage of design hyperspace were generated (Table 5).

Table 5. Possible structural states to create ANN

Training algorithm	Number of Hidden Layers	Number of neurons	Transition function
Trainlm	1	1 st layer: 6 – 8	Tansig
Traingda	2	2 nd layer: 4 – 6	Logsig
Traingdm			Purelin



Every created ANN was trained and tested 3 times with optimum outputs, and after evaluating the average amount of each accuracy estimator parameter (MPE¹, MSE², R-squared³), eventually, the structures with a maximum mean of accuracy were chosen as the best possible structures to predict each output parameter individually. There are various algorithms for training a neural network i.e. gradient descent, Newton method, conjugate gradient, quasi-Newton, and Levenberg-Marquardt. In this research, the Levenberg-Marquardt Algorithm (LMA), which is the fastest method and known as the Damped Least-Squares (DLS), was employed for training, although it usually requires a lot more memory. Hence, the process of randomly reserving 35% of each data for test and training ANN with the remaining ones, was repeated for each structure till achieving accuracy criteria of R²>0.95. The favorite ANN structures and their R-squared amounts after training were shown in Table 6 and the accuracy of trained ANNs could be observed by means of their QQ-plot depicted in Fig. . The developed optimum designer has the ability to predict optimum Bi-lobe tank dimensions for all inexperienced states. The schematics of this process is shown in Fig. 8.

Table 6. Employed ANNs parameters

Output	Training algorithm	Number of Hidden Layers	Number of neurons	Transition function	Coefficient of determination
r	Trainlm	1	7	Tansig	0.9746
a	Trainlm	1	7	Tansig	0.9507
l	Trainlm	2	5,7	Logsig, Tansig	0.9756
t ₁	Trainlm	1	8	Logsig	0.9519
t ₂	Trainlm	1	7	Tansig	0.9749
t ₃	Trainlm	2	4,8	Tansig, Tansig	0.9152
t ₄	Trainlm	2	6,7	Tansig, Logsig	0.9706
Multi objective function	Trainlm	1	8	Logsig	0.9743
Cost function	Trainlm	1	7	Tansig	0.9715
Volume function	Trainlm	1	7	Tansig	0.9838

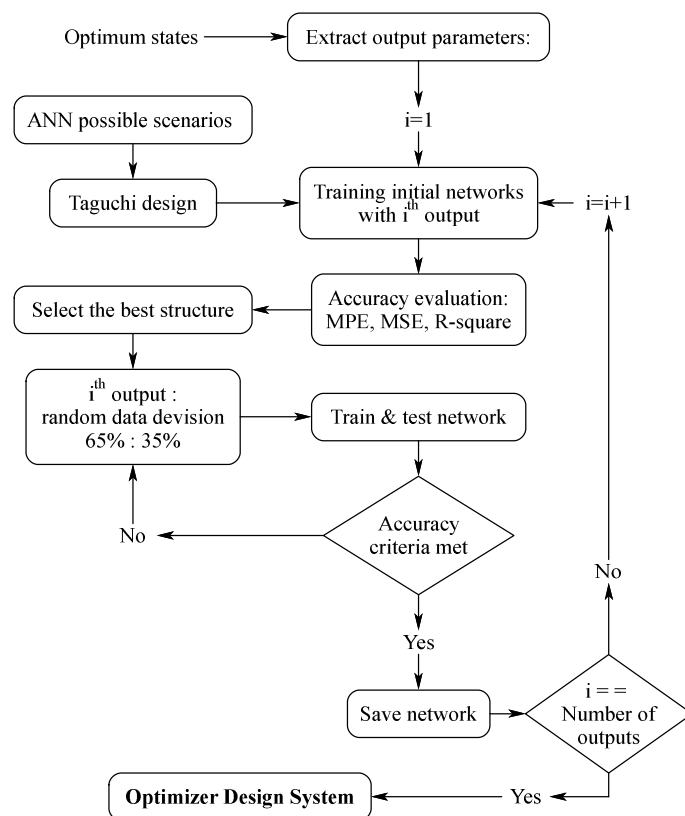


Fig. 8. Mathematical modeling trend

To validate the accuracy of the developed optimum designer system, it was necessary to compare the results with available designs. Consequently, an unexperienced set of design parameters within their permissible ranges was defined and analyzed using GA-FEA, and its optimum design parameters were compared with those predicted by the developed ANNs, as shown in Table 7. The maximum amount of 6.4% error shown in Table 7 depicts the acceptable accuracy of the

¹ Mean Percentage Error (MPE)
² Mean Squared Error (MSE)
³ Coefficient of Determination (R²)

developed design system.

Table 7. Validating ANN results

		W (m)	15.74	
		H (m)	12.11	
		L (m)	39.35	
		Y (°)	140	
		Cost-to-Volume IF	(0.1:0.9)	
		Simulated optimum state	Predicted optimum state	
		Prediction Error (%)		
Inputs	Tank radius (m)	4.7	5.0	6.4
	Deviation (m)	3.15	3.3	4.8
	Shell length (m)	20.1	19.5	3
	Head thickness (mm)	24	26.2	9.2
	Shell thickness (mm)	24	22.8	5
	Stiffener thickness (mm)	25	27.8	11.2
	Bulkhead thickness (mm)	9	9.3	3.3
	Objective function	262021.751	282983.5	8
	Cost function	1709617.871	1589944.6	7
	Volume function	2696.184	2938.8	9
Average prediction error (%)		6.8%		

6. Results and Discussion

In this investigation, more than half a million tanks were generated by GA and about 120000 ones, which had passed dimensional constraints, were analyzed by FEM. Input design parameters and GA results are presented in Appendix A Table A.1.

The results of this study were divided to 3 parts: FEA, GA, and ANNs. Since junctures D, E, F and G in Fig. 3 experience primary local stresses, they were known as critical areas with stress concentration. GA results presented in Appendix A Table A.1 show that by switching volume IF from 0.8 to 1, the required thicknesses increase significantly, because of neglecting cost effect. Besides, in more than 80% of cases, the optimum value of deviation (α) was between 0.35r and 0.80r. Hereafter and before discussing ANN results, it should be noted that all variables have been normalized between 0 to 1 for ANNs to gain a more rational engineering result. Besides, from construction and manufacturing viewpoint and considering commercial sheet thicknesses, the thicknesses and lengths were rounded up with scale of 1mm and 1cm respectively.

Fig. 9 illustrates the effect of each parameter on the objective function, while other parameters were set to the middle of their domains. This figure compares the effect of volume and volume-to-cost IF on the objective function, with up to 35% and 29% influence respectively.

Figure 10 shows the effect of selected inputs within their normalized range on output while 4 other inputs were kept constant at their midrange.

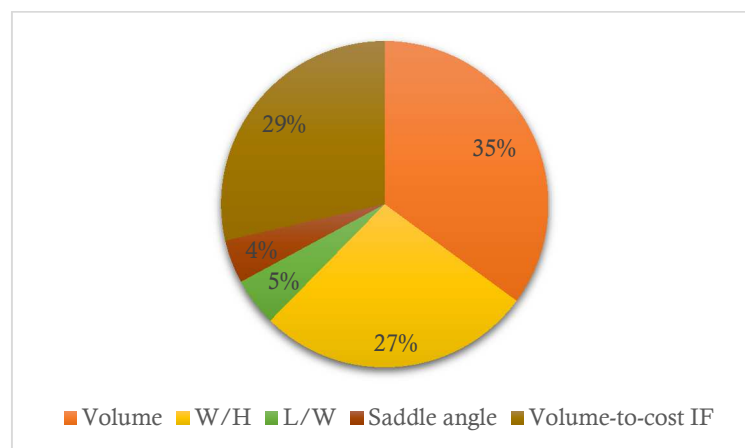


Fig. 9. Parameters effect percentage on objective function

Using 5 specified inputs and ten trained networks predicts one output, the optimal predicted design spaces were 11 unimaginative 6-dimensional hyperspaces. On the other hand, 3D curves could only be implemented to show the effects of a maximum of 3 parameters on output while keeping the rest of variables constant. In Fig. 11, 3D trend of outputs in response to two inputs was shown. By varying the amounts of constant parameters, sets of quadric surfaces completely change. Thus, these charts may be used to point the general behavior of output variables and not just for simple individual analysis. Regarding the number of inputs and outputs, 100 other sets can be plotted to show various responses.

Figure 11.a shows the increasing effect of volume and volume-to-cost IF on the objective function. Figure 11.b shows tank capacity has the main effect on thickness and Fig. 11.c depicts that L/W and W/H do not have a considerable effect on tank thickness.

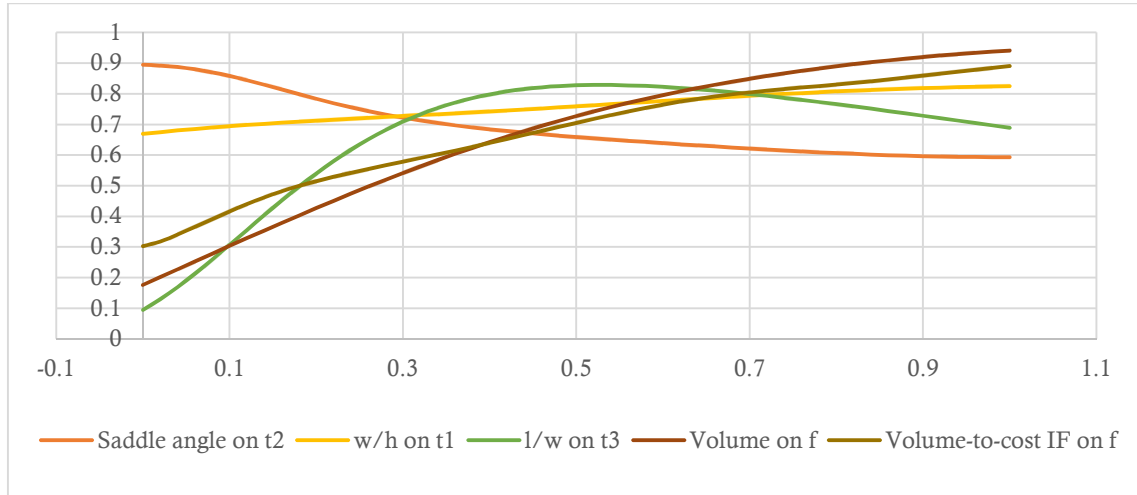


Figure 10. Outputs response to inputs

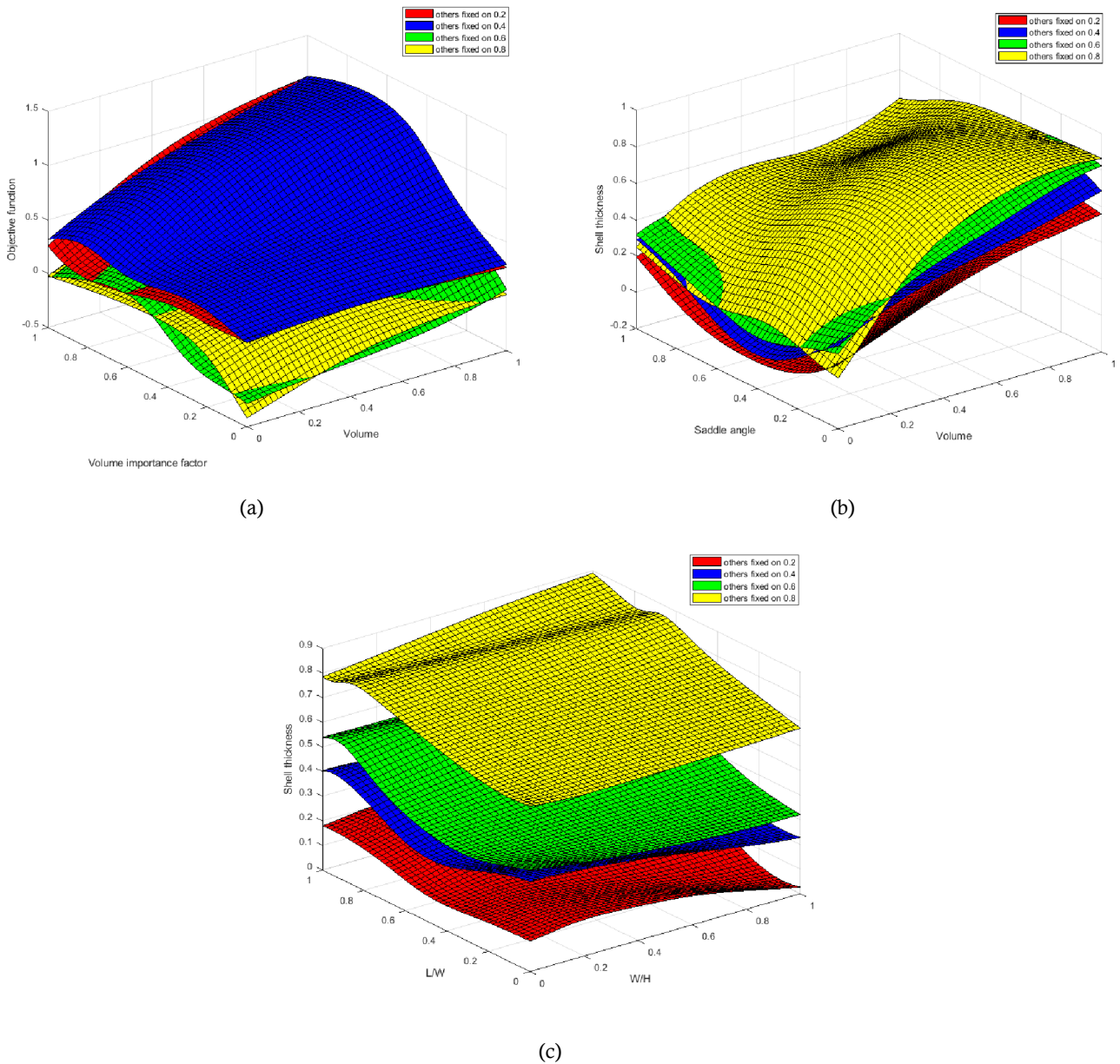


Fig. 11. Output response to multiple inputs

7. Conclusions

A comprehensive study has been conducted for the optimum generation of Bi-lobe tanks for LNG fuel transportation. The developed optimum designer receives dimensions of available space for installing a Bi-lobe tank and suggests designs with maximum volume and best fabricating cost. The most applicable dimensions were considered and the optimum design of tanks was generated using GA and FEA using Python coding in ABAQUS software. The results were then utilized to train 10 ANNs to predict the optimum Bi-lobe dimensions for a new design. Accordingly, the most important results can be summarized as follows:

- The FEA results show that stress concentration occurs in the junctures of shell-shell, horn of saddles, shell-head or head-head. The self-limiting characteristics of stresses at junctures form secondary [48] stresses and beside primary membrane stresses, generate primary local stresses and are allowed to increase up to 1.5 times tank material permissible strength. However, even with this increased amount of permissible strength, it is recommended to use a stiffener ring for saddles.
- GA results show that the best value for the tank deviation parameter (a) is between $0.35r$ and $0.80r$.
- Since stress concentration at the horn of saddle with 120° contact angle is more than other angles, the volume of Bi-lobe tanks with 0.8 IF is much less than the rest. The results also show that lower thicknesses, less volume and reduced amount of cost were obtained by applying cost IF.
- The resultant optimum design parameters of Table 8 lead to the following conclusions:
 1. Increasing saddle angle leads to decrease in stress concentration and therefore a reduction in minimum required shell thickness.
 2. Increasing the cost IF leads to cheaper tank but smaller in capacity.
 3. Escalation of volume leads to more shell thickness and cost, while augmentation of saddle angle reduces the thickness
 4. Optimum saddle angle for smaller tanks is around the midrange (120 to 150), meanwhile, larger tanks require larger saddle angles.
 5. Tanks with higher volume, require more shell thickness. Meanwhile, for the relatively wider tank, the thicker plate is required.

Author Contributions

M. Salarkia reviewed the literature and extracted all the standards, regulations and available design information regarding LNG transportation, performed all the simulations, optimization and finite element results and acquired the main results; S. Golabi supervised the whole research, planned all steps of the project, conducted the design strategy and reviewed and approved the final version of the manuscript, and; B. Amirsalari assisted to develop whole artificial Neural Networks.

Conflict of Interest

The authors declared no potential conflicts of interest with respect to the research, authorship, and publication of this article.

Funding

The authors wish to thank the University of Kashan for supporting this research by grant No. 682570.

Nomenclature

a	Deviation of each tank from the symmetry plane	S_y	Yield Stress
α	Weight importance factor	S_{ut}	Ultimate tensile Stress
β	Volume importance factor	t_1	Head thicknesses
γ	Saddle Angle	t_2	Shell thickness
H	Height of hypothetical rectangular cubes	t_3	Stiffener rings thickness
l'	Shell length	t_4	Longitudinal bulkhead thickness
l	Total length of the tank	V	Tank Volume
L	Length of hypothetical rectangular cubes	w	Tank width
r	Body radius	W	Width of hypothetical rectangular cubes
R^2	Coefficient of determination		

References

- [1] Mokhtab, S., et al., *Handbook of liquefied natural gas*. Gulf Professional Publishing, 2013.




- [2] Adamo, J.D., *On the sustainability of Liquefied Natural Gas (LNG) as a marine fuel in a post-International Maritime Organization (IMO) 0.5% sulfur cap environment*. Ph.D. Thesis, The University of Texas at Austin, USA, 2018.
- [3] Arteconi, A., et al., Life-cycle greenhouse gas analysis of LNG as a heavy vehicle fuel in Europe. *Applied Energy*, 87(6), 2010, 2005-2013.
- [4] Schinas, O. and M. Butler, Feasibility and commercial considerations of LNG-fueled ships. *Ocean Engineering*, 122, 2016, 84-96.
- [5] Baumgart, M. and J.H.B. Olsen, *LNG-fueled vessels in the Norwegian short-sea market: a cost-effective response to environmental regulation*. Master Thesis, 2010.
- [6] Thomson, H., J.J. Corbett, and J.J. Winebrake, Natural gas as a marine fuel. *Energy Policy*, 87, 2015, 153-167.
- [7] Bengtsson, S., K. Andersson, and E. Fridell, A comparative life cycle assessment of marine fuels: liquefied natural gas and three other fossil fuels. *Proceedings of the Institution of Mechanical Engineers, Part M: Journal of Engineering for the Maritime Environment*, 225(2), 2011, 97-110.
- [8] Brynolf, S., E. Fridell, and K. Andersson, Environmental assessment of marine fuels: liquefied natural gas, liquefied biogas, methanol and bio-methanol. *Journal of Cleaner Production*, 74, 2014, 86-95.
- [9] Lowell, D., H. Wang, and N. Lutsey, Assessment of the fuel cycle impact of liquefied natural gas as used in international shipping. *The International Council on Clean Transportation*, Washington, DC, 2013.
- [10] Roy, B. and B. Comer, Alternatives to heavy fuel oil use in the Arctic: Economic and environmental tradeoffs. *The International Council on Clean Transportation*, Working Paper, 4, 2017, 2017p.
- [11] Wood, D.A., A review and outlook for the global LNG trade. *Journal of Natural Gas Science and Engineering*, 9, 2012, 16-27.
- [12] Al Ali, M., *Development of novel energy systems for LNG locomotives*. Master Thesis, University of Ontario Institute of Technology Oshawa, Ontario, Canada, 2015.
- [13] Iden, M.E. Liquefied Natural Gas (LNG) as a Freight Railroad Fuel: Perspective from a Western US Railroad. in *ASME 2012 Rail Transportation Division Fall Technical Conference*, American Society of Mechanical Engineers, 2012.
- [14] Hagos, D.A. and E.O. Ahlgren, Well-to-wheel assessment of natural gas vehicles and their fuel supply infrastructures—Perspectives on gas in transport in Denmark. *Transportation Research Part D: Transport and Environment*, 65, 2018, 14-35.
- [15] Osorio-Tejada, J.L., E. Llera-Sastresa, and S. Scarpellini, Liquefied natural gas: Could it be a reliable option for road freight transport in the EU?. *Renewable and Sustainable Energy Reviews*, 71, 2017, 785-795.
- [16] Delgado, O. and R. Muncrief, Assessment of heavy-duty natural gas vehicle emissions: implications and policy recommendations. *White Paper*, 2015.
- [17] Le Fevre, C.N., *A review of demand prospects for LNG as a marine fuel*. Oxford Institute for Energy Studies, 2018.
- [18] Adamchak, F. and A. Adede. LNG as marine fuel. in *17th International Conference & Exhibition*, 2013.
- [19] Baresic, D., et al., *LNG as a marine fuel in the EU. Market, bunkering infrastructure investments and risks in the context of GHG reductions*. Master Thesis, University Maritime Advisory Services, 2018.
- [20] McGill, R., W. Remley, and K. Winther, Alternative fuels for marine applications. *A Report from the IEA Advanced Motor Fuels Implementing Agreement*, 2013.
- [21] Kotwzan, K. and M. Narewski, Alternative fuels for marine applications. *Latvian Journal of Chemistry*, 51(4), 2012, 398-406.
- [22] Sharafian, A., et al., A review of liquefied natural gas refueling station designs. *Renewable and Sustainable Energy Reviews*, 69, 2017, 503-513.
- [23] Shin, S.-H. and D.-E. Ko, A study on forces generated on spherical type LNG tank with central cylindrical part under various static loading. *International Journal of Naval Architecture and Ocean Engineering*, 8(6), 2016, 530-536.
- [24] Zhang, C., et al., A large LNG tank technology system “CGTank®” of CNOOC and its engineering application. *Natural Gas Industry B*, 2(6), 2015, 530-534.
- [25] Morimoto, N., *LNG tanker and method for marine transportation of Ing*. Google Patents, 2010.
- [26] Ryu, M.C., et al., Sloshing design load prediction of a membrane type LNG cargo containment system with two-row tank arrangement in offshore applications. *International Journal of Naval Architecture and Ocean Engineering*, 8(6), 2016, 537-553.
- [27] Arswendy, A. and T. Moan, Strength and stiffness assessment of an LNG containment system—Crushing and buckling failure analysis of plywood components. *Engineering Failure Analysis*, 48, 2015, 247-258.
- [28] Ishimaru, J., et al., Building of advanced large sized membrane type LNG carrier. *Mitsubishi Heavy Industries Technical Review*, 41(6), 2004, 1-10.
- [29] Limited, L.s.R.G., ShipRight Design and Construction, in Primary Hull and Cargo Tank Supporting Structure of Type C Tank Liquefied Gas Carriers. 2017, Lloyd's Register Group Limited: 71 Fenchurch Street, London. p. 73.
- [30] Strength Analysis of Independent Type C Tanks. - Classification Notes No. 31.13, DNV, 2013.
- [31] Lamb, T., *Ship design and construction*. Vol. I., The Society of Naval Architects and Marine Engineers, 2003.
- [32] Senjanović, I., et al. Structure design of cargo tanks in liquefied gas carriers. in *International Congress of Marine Research and Transportation*, ICMRT 2005, 2005.
- [33] *BP statistical review of world Energy*, 2018.
- [34] *Rules for Building and classing, Steel vessels*, in part 5C. American Bureau of Shipping (ABS). 2008, p. 981-982.
- [35] Vyas, N., A techno-economic study of liquefied natural gas transportation: a prospective to develop India's first import


terminal. World Maritime University, Sweden, 2000.

- [36] Kokarakis, J., *Standard and Guidelines for Natural Gas Fuelled Ship Projects*. University of Strathclyde, 2015, 9-87.
- [37] Harperscheidt, J. LNG as Fuel–Bunkering, storage and processing. in *STG International Conference Ship Efficiency*, Hamburg, Germany, 2011.
- [38] Harperscheidt, J., Bunkering, infrastructure, storage, and processing of LNG. *Ship & Offshore*, 1(1), 2011, 12-15.
- [39] Wang, B., Y.-S. Shin, and X. Wang. Structural integrity assessment of independent type ‘C’ LNG carriers. in *ASME 2014 33rd International Conference on Ocean, Offshore and Arctic Engineering*, American Society of Mechanical Engineers, 2014.
- [40] ASME Boiler and Pressure Vessel Code, An International Code Sec II Part D, 2015 ed. Part D Properties (Customary). 2015, New York, USA: The American Society of Mechanical Engineers. 923.
- [41] Code, I., International code for the construction and equipment of ships carrying liquefied gases in bulk. *International Maritime Organization*, 2003.
- [42] Kumar, V., et al., Design of Saddle Support for Horizontal Pressure Vessel. *International Journal of Mechanical, Aerospace, Industrial, Mechatronic and Manufacturing Engineering*, 8(12), 2014, 1-5.
- [43] Yao, Y. and G. Zhongyun. The structure design of type-C independent tank on LNG ship. in *The 2015 World Congress on Advances in Structural Engineering and Mechanics*, Incheon, Korea, 2015.
- [44] Shin, S.-B., et al. A Study on Design of IMO C type LNG Fuel Storage Tank With Capacity of 500m³. in *The Twenty-third International Offshore and Polar Engineering Conference*, International Society of Offshore and Polar Engineers, 2013.
- [45] Senjanović, I., J. Parunov, and S. Rudan, Remedy for Misalignment of Bilobe Tank Heads in Liquefied Petroleum Gas Carrier. *Brodogradnja: Teorija i Praksa Brodogradnje i Pomorske Tehnike*, 60(3), 2009, 290-297.
- [46] Claudepierre, M. IGF Code Update & LNG Bunkering Guidelines. 2014, Available from: <https://docplayer.net/20908063-Igf-code-update-lng-bunkering-guidelines.html>.
- [47] Munko, B., Economic design of small scale LNG tankers and terminals. in *TGE Gas Engineering, LNG Conference*, Offshore Center Denmark, 2007.
- [48] Moss, D.R., Pressure Vessel Design Manual. Fourth edition, Oxford, UK, Elsevier, 2013.
- [49] Smith, L. and B. Craig, Properties of metallic materials for LNG service. *Stainless Steel World*, 13, 2001, 27-32.
- [50] Toussaint, P. Development of Materials of construction for the new challenges and processes of the LNG chain. in *LNG 17 International Conference & Exhibition on LNG*, 2013.
- [51] USCG, Safety Standards for self-propelled Vessels carrying Bulk Liquefied Gases, 46 CFR (Code of Federal Register), in Part 154, § 154.170/172/176. 2017.

ORCID iD

Mohammadreza Salarkia  <https://orcid.org/0000-0001-6143-0651>

Sa'id Golabi  <https://orcid.org/0000-0000-3178-1023>

Behzad Amirjalali  <https://orcid.org/0000-0002-4395-9559>

Appendix A

Table A.1. Optimum states generated by GA

No	W (m)	H (m)	L (m)	γ (°)	Volume importance factor	r (m)	a (m)	l' (m)	t ₁ (mm)	t ₂ (mm)	t ₃ (mm)	t ₄ (mm)	Objective function	Cost function	Volume function
1	6.2996	6.2996	12.5992	120	0.8	1.95	1.05	8.65	8	8	6	3	24106.492	92895.95	190.561
2	11.4471	11.4471	22.8943	120	0.8	3.2	2.25	13.7	17	13	23	5	95643.379	397813.7	888.678
3	14.4225	14.4225	28.845	120	0.8	4.8	2.15	16.45	21	21	20	7	253804.87	1184841	2190.951
4	16.5096	16.5096	33.0193	120	0.8	5.05	3.05	16.55	29	24	49	8	224021.61	1773303	2583.402
5	5.5032	5.5032	16.5096	120	0.8	1.6	1.05	12.7	8	8	5	3	21119.687	106509.7	189.382
6	10	10	30	120	0.8	2.85	2.1	16.2	25	15	22	5	63886.911	576433.3	799.882
7	12.5992	12.5992	37.7976	120	0.8	4.2	2.05	16.25	21	20	17	7	177682.21	964714.5	1654.576
8	14.4225	14.4225	43.2675	120	0.8	4.8	2.2	19.75	29	28	18	10	220339.93	1780241	2573.162
9	5	5	20	120	0.8	1.4	1.05	13.55	6	6	5	3	19974.116	77438.06	159.05
10	9.0856	9.0856	36.3424	120	0.8	3.4	1.05	16.3	16	16	10	6	110047.37	529982.5	964.482
11	11.4471	11.4471	45.7886	120	0.8	3.4	2.05	16.5	18	15	26	5	120093.98	656747.7	1122.516
12	13.1037	13.1037	52.4148	120	0.8	4.2	2.3	17.3	21	21	20	7	182209.52	1091867	1788.317
13	7.2112	4.8075	14.4225	120	0.8	2.3	1.3	9.65	7	7	6	3	45172.891	110641.2	300.456
14	13.1037	8.7358	26.2074	120	0.8	3.55	1.85	13.2	14	13	13	5	128885.84	450139.8	977.294
15	16.5096	11.0064	33.0193	120	0.8	5.45	2.1	17.9	26	26	23	9	322163.86	1766508	3015.471
16	18.8988	12.5992	37.7976	120	0.8	6.25	2.25	18.5	33	33	26	11	392641.43	2668762	4135.687
17	6.2996	4.1997	18.8988	120	0.8	1.9	1.15	12.5	7	7	7	3	35743.277	112535.8	260.047
18	11.4471	7.6314	34.3414	120	0.8	3.55	2.15	16.6	16	16	25	6	135161.57	708707	1236.174
19	14.4225	9.615	43.2675	120	0.8	4.7	2.1	17.65	22	21	25	7	245832.45	1259271	2221.816
20	16.5096	11.0064	49.5289	120	0.8	4.9	2.3	20.45	30	30	19	10	222870.75	2004594	2784.775
21	5.7236	3.8157	22.8943	120	0.8	1.8	0.95	16.45	8	8	10	3	34669.197	152024.3	290.509
22	10.4004	6.9336	41.6017	120	0.8	3.35	1.75	16.15	13	13	28	5	124334.99	536789.5	1034.343
23	13.1037	8.7358	52.4148	120	0.8	4.25	1.6	19.45	25	25	11	9	169055.52	1262256	1881.726
24	15	10	60	120	0.8	4.95	2.35	20.55	30	30	21	10	230237.63	2056819	2683.675
25	7.937	3.9685	15.874	120	0.8	1.85	1.25	12.1	7	7	6	3	33274.411	108310.1	245.252
26	14.4225	7.2112	28.845	120	0.8	3.55	2.15	12.05	11	11	27	4	126006.33	407260.3	926.153
27	18.1712	9.0856	36.3424	120	0.8	4.5	2.3	17.35	31	25	23	9	166701.44	1317368	2071.992
28	20.8008	10.4004	41.6017	120	0.8	4.75	2.35	16.75	44	27	23	9	144963.91	1088979	2189.025

29	6.9336	3.4668	20.8008	120	0.8	1.7	1	11.6	8	6	9	3	25687.931	85895.63	191.371
30	12.5992	6.2996	37.7976	120	0.8	3	1.35	17.75	16	13	21	5	95816.555	487805.6	863.293
31	15.874	7.937	47.622	120	0.8	3.75	2.05	18.6	22	21	17	7	136027.7	1003967	1503.666
32	18.1712	9.0856	54.5136	120	0.8	4.45	2	19.15	22	22	26	8	215135.03	1302556	2123.421
33	6.2996	3.1498	25.1984	120	0.8	1.5	1.2	14.55	7	7	11	3	22423.885	110956.7	199.175
34	11.4471	5.7236	45.7886	120	0.8	2.8	1.7	17.1	14	13	25	5	81223.889	463974	776.869
35	14.4225	7.2112	57.69	120	0.8	3.55	1.85	20.65	21	21	23	7	120075.69	1033372	1458.705
36	16.5096	8.2548	66.0385	120	0.8	3.95	1.55	25.5	29	27	29	9	120252.9	1710784	2064.329
37	6.2996	6.2996	12.5992	120	1	2	1.1	8.55	13	7	19	3	55940.564	112697.1	199.788
38	11.4471	11.4471	22.8943	120	1	3.45	2.1	15.5	47	20	31	7	306615.46	1003925	1095.055
39	14.4225	14.4225	28.845	120	1	4.5	2.65	19.65	42	36	28	12	658585.53	2328600	2352.091
40	16.5096	16.5096	33.0193	120	1	4.9	3.3	22.85	47	42	47	14	927745.03	3584068	3313.375
41	5.5032	5.5032	16.5096	120	1	1.55	1.15	13.3	12	10	6	4	53620.295	142556.7	191.501
42	10	10	30	120	1	2.9	2.05	23.95	38	10	28	4	334346.85	686984.9	1194.096
43	12.5992	12.5992	37.7976	120	1	4.15	2.05	29.45	49	48	19	16	773096.69	3533035	2761.059
44	14.4225	14.4225	43.2675	120	1	4.85	2.25	29.9	48	45	27	15	1067833.5	4064255	3813.691
45	5	5	20	120	1	1.35	1.1	14.65	41	10	7	4	45581.571	174835	162.791
46	9.0856	9.0856	36.3424	120	1	3.25	1.25	26.7	41	28	9	10	398969.8	1412836	1424.892
47	11.4471	11.4471	45.7886	120	1	3.15	2.55	34.1	49	43	27	9	576778.55	3206156	2059.923
48	13.1037	13.1037	52.4148	120	1	4.45	2.05	32.6	48	47	30	16	964263.66	4123113	3443.799
49	7.2112	4.8075	14.4225	120	1	2.35	1.2	9.7	12	7	18	3	86649.661	145451.8	309.463
50	13.1037	8.7358	26.2074	120	1	4.3	2.2	17.35	48	27	27	9	520530.47	1651350	1859.037
51	16.5096	11.0064	33.0193	120	1	5.3	2.9	22.15	46	34	30	12	1019118.1	3023515	3639.708
52	18.8988	12.5992	37.7976	120	1	6.25	3.1	23.85	50	47	28	16	1513122.6	4874987	5404.009
53	6.2996	4.1997	18.8988	120	1	1.85	1.25	14.95	27	11	17	4	84023.927	249198.5	300.085
54	11.4471	7.6314	34.3414	120	1	3.75	1.9	26	47	38	25	13	561901.73	2377999	2006.792
55	14.4225	9.615	43.2675	120	1	4.35	2.7	29.7	47	44	30	15	910556.56	3787612	3251.988
56	16.5096	11.0064	49.5289	120	1	4.75	3.25	23.25	42	40	27	14	886945.35	3948636	3747.548
57	5.7236	3.8157	22.8943	120	1	1.85	0.8	13.6	47	15	4	5	68406.978	210634.6	303.291
58	10.4004	6.9336	41.6017	120	1	3.3	1.9	30.35	45	42	29	14	516631.92	2639479	1845.114
59	13.1037	8.7358	52.4148	120	1	3.9	2.35	34.95	49	49	26	17	842577.94	4167883	3009.207
60	15	10	60	120	1	4.5	2.8	30.2	47	46	29	16	992440.46	4135275	3544.43
61	7.937	3.9685	15.874	120	1	1.95	1.55	11.95	31	14	7	5	78262.372	279513.7	279.508
62	14.4225	7.2112	28.845	120	1	3.55	3.05	21.6	47	31	28	11	475047.72	1961300	1696.599
63	18.1712	9.0856	36.3424	120	1	4.35	2.6	22.15	47	37	16	13	686641.89	4157668	3329.67
64	20.8008	10.4004	41.6017	120	1	4.9	3.35	24.65	43	42	30	14	998767.51	3652512	3567.027
65	6.9336	3.4668	20.8008	120	1	1.7	1.45	17.25	32	10	26	4	86064.702	270889.9	307.374
66	12.5992	6.2996	37.7976	120	1	3.1	2.4	31.4	47	46	24	16	509499.44	3017102	1819.641
67	15.874	7.937	47.622	120	1	3.75	3.1	29.35	49	49	14	17	711419.97	3797471	2540.786
68	18.1712	9.0856	54.5136	120	1	4.5	3.4	26.05	49	48	29	16	901661.06	4062372	3220.218
69	6.2996	3.1498	25.1984	120	1	1.5	1.25	16.35	31	8	8	3	63124.374	174315.8	225.444
70	11.4471	5.7236	45.7886	120	1	2.8	2.4	30.85	49	42	13	14	417498.31	2551896	1491.065
71	14.4225	7.2112	57.69	120	1	3.55	2.7	35.2	50	50	29	17	746055.27	4194648	2664.483
72	16.5096	8.2548	66.0385	120	1	4.1	3.35	30.5	50	50	23	17	882755.52	4447146	3152.698
73	6.2996	6.2996	12.5992	150	0.8	2	1.1	8.55	6	6	5	3	30329.012	72117.2	199.788
74	11.4471	11.4471	22.8943	150	0.8	3.65	2.05	15.5	17	17	9	6	139203.24	661765.8	1212.305
75	14.4225	14.4225	28.845	150	0.8	4.8	2.25	19.5	25	25	11	9	260579.07	1515518	2516.44
76	16.5096	16.5096	33.0193	150	0.8	5.15	3.05	21.5	23	22	36	8	380676.7	1892402	3389.095
77	5.5032	5.5032	16.5096	150	0.8	1.6	1.1	11.75	7	7	5	3	22046.279	89037.33	177.918
78	10	10	30	150	0.8	2.85	2.1	22.45	15	14	27	5	111028.75	670194.8	1094.052
79	12.5992	12.5992	37.7976	150	0.8	4	2.25	21.45	19	18	20	6	225649.79	1080599	1972.185
80	14.4225	14.4225	43.2675	150	0.8	4.75	2.4	21.1	23	23	13	8	302832.74	1533434	2721.069
81	5	5	20	150	0.8	1.35	1.1	14.7	6	6	5	3	20042.784	82723.82	163.337
82	9.0856	9.0856	36.3424	150	0.8	3.35	1.15	20.95	16	14	21	5	137684.82	641949.3	1187.833
83	11.4471	11.4471	45.7886	150	0.8	4.3	2.1	17.45	20	17	10	6	236533.49	890652.8	1851.179
84	13.1037	13.1037	52.4148	150	0.8	4.35	2.15	23	20	20	23	7	273046.84	1356957	3430.528
85	7.2112	4.8075	14.4225	150	0.8	2.35	1.2	9.7	7	7	6	3	47070.274	111247.3	309.463
86	13.1037	8.7358	26.2074	150	0.8	3.8	2.65	18.4	20	17	16	6	179835.24	450139.8	1611.544
87	16.5096	11.0064	33.0193	150	0.8	5.35	2.2	22	26	25	17	9	393071.34	1937911	3485.061
88	18.8988	12.5992	37.7976	150	0.8	6.15	2.7	22.05	32	31	21	11	489904.49	2892843	4769.969
89	6.2996	4.1997	18.8988	150	0.8	2	1.1	14.85	8	8	5	3	44416.554	149149.9	331.458
90	11.4471	7.6314	34.3414	150	0.8	3.75	1.9	24.55	25	20	12	7	188545.04	1188916	1903.251
91	14.4225	9.615	43.2675	150	0.8	4.7	2.35	27.9	28	28	28	10	287345.82	2387317	3414.327
92	16.5096	11.0064	49.5289	150	0.8	5.4	2.55	20.85	27	26	14	9	384315.79	1984883	3487.912
93	5.7236	3.8157	22.8943	150	0.8	1.85	0.9	16.2	8	8	4	3	38127.222	141206.5	296.288
94	10.4004	6.9336	41.6017	150	0.8	3.3	1.9	25.15	20	17	25	6	149781.24	980833.5	1544.41
95	13.1037	8.7358	52.4148	150	0.8	4.05	2.4	23.35	23	23	14	8	207223.84	1445077	2215.354
96	15	10	60	150	0.8	4.95	2.4	22.2	27	24	15	8	332645.21	1784981	3078.756
97	7.937	3.9685	15.874	150	0.8	1.95	1.5	11.75	7	7	8	3	37346.721	119329.5	273.271
98	14.4225	7.2112	28.845	150	0.8	3.5	1.95	14.5	12	12	20	4	140744.17	465357.7	1043.82
99	18.1712	9.0856	36.3424	150	0.8	4.5	2.2	24.1	48	23	27	8	214230.59	1651919	2746.211
100	20.8008	10.4004	41.6017	150	0.8	5.1	2.45	22.25	32	24	17	8	347054.7	1938188	3279.876
101	6.9336	3.4668	20.8008	150	0.8	1.65	0.9	13.5	6	6	4	3	28966.338	83004.57	203.425
102	12.5992	6.2996	37.7976	150	0.8	3.1	2	27.35	18	18	28	6	128744.79	1055408	1517.082
103	15.874	7.937	47.622	150	0.8	3.75	2.3	22.45	21	19	18	7	188397.8	1114683	1836.314
104	18.1712	9.0856	54.5136	150	0.8	4.45	2.2	22.9	24	22	16	8	271261.61	1487929	2539.497
105	6.2996	3.1498	25.1984	150	0.8	1.5	1.2	13.5	6	6	8	3	23255.913	85783.18	180.413
106	11.4471	5.7236	45.7886	150	0.8	2.75	1.9	22.15	15	14	19	5	100802.37	602795.4	988.221
107	14.4225	7.2112	57.69	150	0.8	3.55	2	23.35	17	17	22	6	180857.19	961154.6	1665.572
108	16.5096	8.2548	66.0385	150	0.8	4.1	2.15	22.25	20	20	17	7	230642.18	1212659	2112.383
109	6.2996	6.2996	12.5992	150	1	2	1								

113	5.5032	5.5032	16.5096	150	1	1.6	1.1	13.25	50	50	5	1.7	55898.703	674228.5	199.638
114	10	10	30	150	1	2.8	2.15	24.35	41	20	20	7	322915.28	1065525	1153.269
115	12.5992	12.5992	37.7976	150	1	3.6	2.65	30.5	46	45	15	15	662283.89	3285297	2365.299
116	14.4225	14.4225	43.2675	150	1	4.85	2.35	33	48	38	27	13	1181245.7	3907209	4218.735
117	5	5	20	150	1	1.4	1.05	14.7	38	8	11	3	48213.419	153469.8	172.191
118	9.0856	9.0856	36.3424	150	1	3.3	1.15	26.55	44	26	27	9	400215.12	1443843	1429.339
119	11.4471	11.4471	45.7886	150	1	3.45	2.2	33.7	49	35	29	12	643528.71	2724761	2298.317
120	13.1037	13.1037	52.4148	150	1	3.8	2.7	37.75	45	37	26	13	900523.3	3575544	3216.154
121	7.2112	4.8075	14.4225	150	1	2.25	1.3	9.8	33	7	22	3	81816.035	209599.7	292.2
122	13.1037	8.7358	26.2074	150	1	4.3	2.2	17.45	50	20	11	7	1333023.6	1353518	1868.458
123	16.5096	11.0064	33.0193	150	1	5.15	3.05	22.55	43	29	19	10	990770.16	2585209	3538.465
124	18.8988	12.5992	37.7976	150	1	6	3.4	25.75	48	46	15	16	1524919.5	4841308	5446.141
125	6.2996	4.1997	18.8988	150	1	2.05	1.05	14.5	37	14	5	5	93770.847	306125.2	334.896
126	11.4471	7.6314	34.3414	150	1	3.65	2.05	26.6	43	27	10	9	557396.82	1744802	1990.703
127	14.4225	9.615	43.2675	150	1	4.75	2.2	33.05	46	38	29	13	1119944	3773929	3999.8
128	16.5096	11.0064	49.5289	150	1	5.2	3	34	48	45	20	15	1466337.7	5115186	5236.92
129	5.7236	3.8157	22.8943	150	1	1.85	0.95	16.75	36	9	14	3	86877.031	235479.5	310.275
130	10.4004	6.9336	41.6017	150	1	3.4	1.75	29.4	44	32	8	11	516772.1	1944777	1845.615
131	13.1037	8.7358	52.4148	150	1	4.15	2.35	37.6	45	44	23	15	1008296.4	4210034	3601.058
132	15	10	60	150	1	4.75	2.4	40.55	48	47	19	16	1385248.2	5358758	4947.315
133	7.937	3.9685	15.874	150	1	1.95	1.7	11.85	39	9	28	3	78794.618	255461.6	281.409
134	14.4225	7.2112	28.845	150	1	3.35	2.05	21.8	39	16	25	6	396111.23	1841298	1640.638
135	18.1712	9.0856	36.3424	150	1	4.5	3.7	26.8	49	34	30	12	941176.9	3295496	3361.346
136	20.8008	10.4004	41.6017	150	1	5.1	4.55	31.1	50	48	29	16	1418424.3	5907689	5065.801
137	6.9336	3.4668	20.8008	150	1	1.7	1.5	17.4	31	14	7	5	87375.454	330975.8	312.055
138	12.5992	6.2996	37.7976	150	1	3.05	2.65	31.65	42	37	12	13	510014.99	2542766	1821.482
139	15.874	7.937	47.622	150	1	3.7	3	39.6	42	40	30	14	924665.84	4069942	3302.378
140	18.1712	9.0856	54.5136	150	1	4.45	3.1	38.95	48	47	26	16	1272824	5365751	4545.8
141	6.2996	3.1498	25.1984	150	1	1.5	1.35	17	30	8	21	3	66626.787	193520.5	237.953
142	11.4471	5.7236	45.7886	150	1	2.4	2.4	29.95	45	25	12	9	405478.31	1577428	1448.137
143	14.4225	7.2112	57.69	150	1	3.55	3.15	37.8	47	40	25	14	828212.15	3921646	2957.901
144	16.5096	8.2548	66.0385	150	1	4.05	3.3	38.5	49	43	26	15	1080742.8	4730146	3859.796



© 2020 by the authors. Licensee SCU, Ahvaz, Iran. This article is an open-access article distributed under the terms and conditions of the Creative Commons Attribution-NonCommercial 4.0 International (CC BY-NC 4.0 license) (<http://creativecommons.org/licenses/by-nc/4.0/>).